Three-nucleon potential effects in spin observables of elastic deuteron-proton scattering

Amir-Ahmadi, Hamid Reza

3. Experimental setup

The study of the reaction $\mathrm{H}(\vec{d}, \vec{p})d$ was performed at Kernfysisch Versneller Instituut (KVI), using the Big-Bite Spectrometer (BBS). The incident beam of 180 MeV polarized deuterons was provided by the superconducting cyclotron AGOR. At KVI, the POLarized Ion Source (POLIS) is used to produce polarized proton and deuteron beams. Figure 3.1 shows the AGOR cyclotron, POLIS, and other experimental facilities at KVI as they were in 2004.

In order to study the polarization-transfer observables of the reaction $\mathrm{H}(\vec{d}, \vec{p})d$, the polarization of the incoming and the outgoing particles have to be measured. The polarization of the proton and deuteron beams emerging from AGOR can be measured using the In-Beam polarimeter (IBP). A Lamb-Shift Polarimeter (LSP) can be employed to measure the polarization of the beam before injecting to AGOR. The polarization of the outgoing protons was measured with the polarimeter of the BBS. To use the BBS for such an experiment, the detector had to be calibrated for proton polarization measurement. This calibration was performed by using the reaction $\mathrm{H}(\vec{p}, \vec{p})p$ with 190 MeV polarized proton beam. These experiments were performed in parts in 2002 and 2005. In this chapter the various parts of the experimental setup used for this experiment will be discussed.

3.1 The polarized ion source

The POLarized Ion Source (POLIS) is an atomic beam source which is able to produce polarized protons and deuterons [59, 60]. The source consists of an atomic jet, providing an atomic hydrogen (or deuterium) beam by means of an RF-induced discharge. This beam passes through two hexapole lenses where the atoms with positive electron polarization ($m_j = +1/2$) are focused toward Radio Frequency (RF) transition units while atoms with negative electron polarization are defocused. Each transition unit consists of a solenoid followed by an RF cavity which is inside a permanent dipole magnet with a certain gradient.

The electron and nucleus spins are coupled to give the total angular momentum J (J=1, 0 for hydrogen and J=3/2, 1/2 for deuterium) [61]. An external magnetic field removes the degeneracy of the energy levels, making it possible to induce transitions between the sub-states by appropriate RF fields, as illustrated in Fig. 3.2.

The ionizer is down-stream of the transition units and hexapoles. It is an RF field of 2.54 GHz, and has a magnetic field between 125 and 200 mT. Therefore,
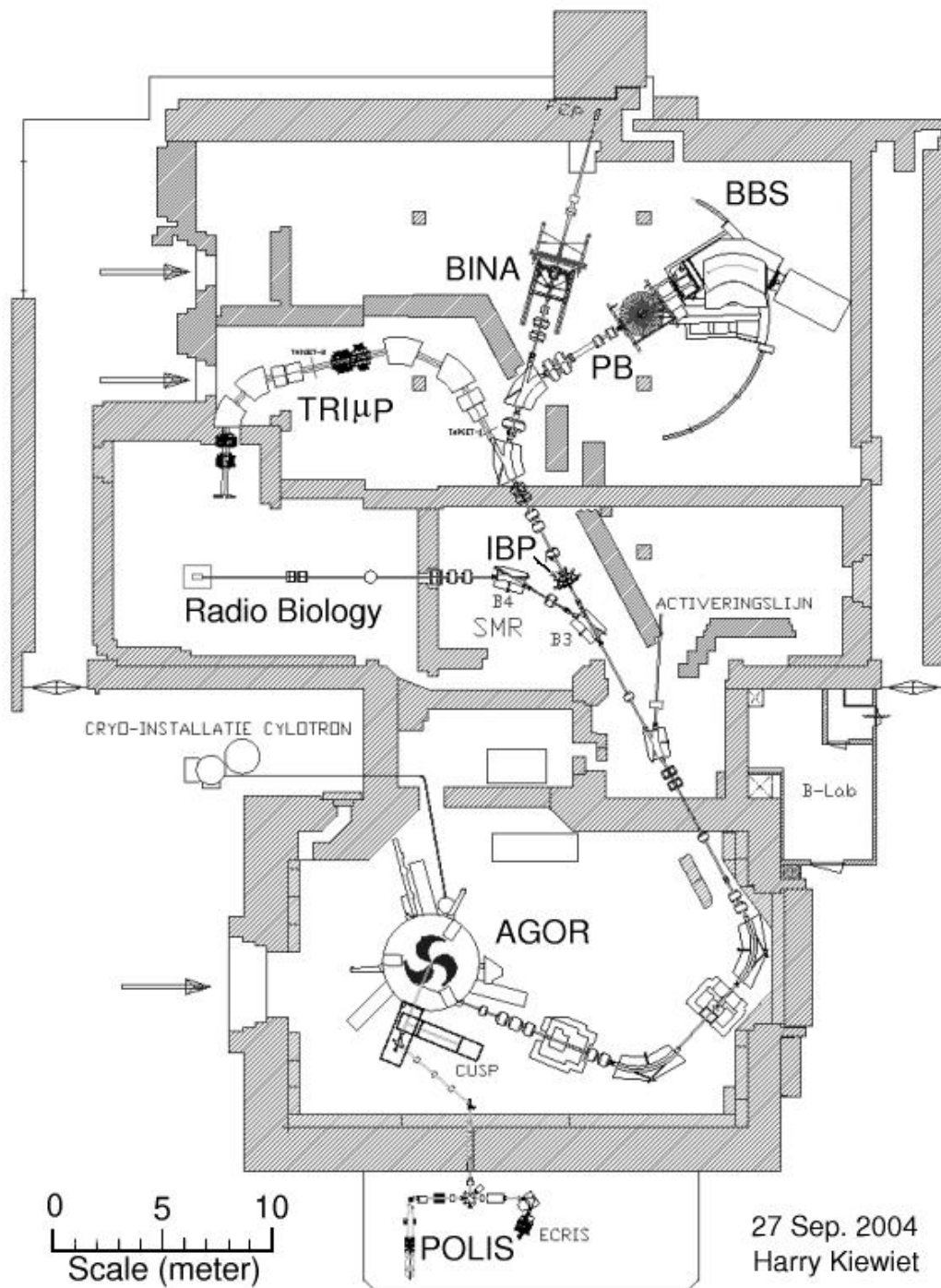
Figure 3.1: Schematic diagram of the cyclotron vault, the experimental areas and experimental facilities; 2004.
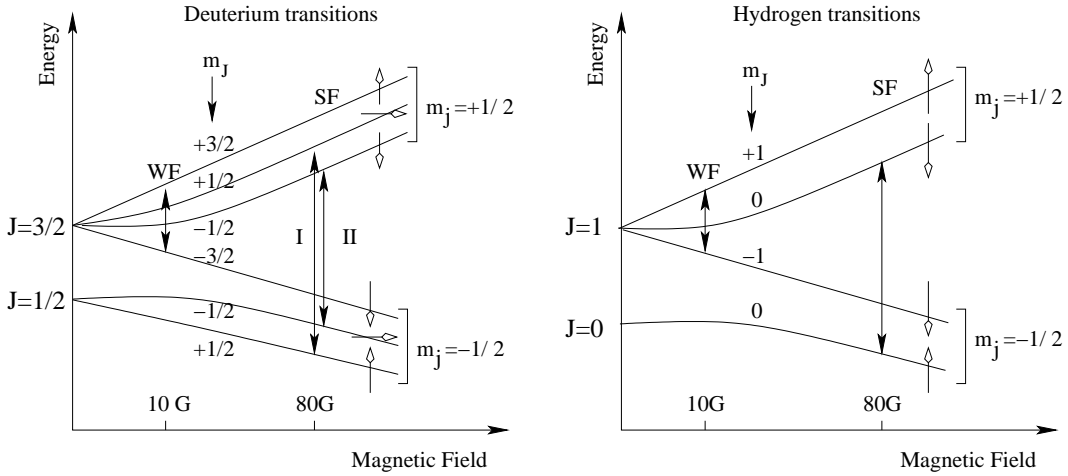
Figure 3.2: Schematic diagram of the hyperfine structure of deuterium (left) and hydrogen (right). The external magnetic field removes the degeneracy of the energy levels. Atoms with spin-up electrons are focused whereas atoms with spin-down electrons are defocused.

the ionizer field induces a transition, causing non-zero polarization of the beam even when all the transition units are off. This is referred to as the polarization-off in this thesis. This non-zero polarization is larger for protons than deuterons due to the large difference in the respective magnetic moments. To obtain a completely unpolarized beam, it is necessary to switch off both RF transition units and the hexapoles [61].

3.1.1 Proton polarization

A so-called weak field (WF) of 7 MHz at a low magnetic field of about 1 mT induces transitions between hyper-fine structure states with equal total angular momentum and opposite magnetic quantum number ($\Delta J = 0, m_J \rightarrow -m_J$). The weak field leaves the other states untouched. In this way, the majority of the protons will have their spin pointing downwards (spin-down protons).

In order to increase the population of the protons with their spin pointing upwards (spin-up protons), a strong field (SF) transition at a magnetic field of about 8 mT is needed. Applying this strong field of 1.4 GHz induces a transition between hyper-fine structure states with different total angular momentum and equal magnetic quantum number ($\Delta J = 1, \Delta m_J = 0$). Figure 3.2 shows all possible transitions for hydrogen and deuterium.

Table 3.1: The polarization degrees of deuterons which are used in this experiment.

Field(s)	p_z	p_{zz}	
WF	$-2/3$	0	pure vector down
SFI+SFII	$+2/3$	0	pure vector up
MF+SFII	0	-2	pure tensor down
MF+SFI	0	$+1$	pure tensor up
unpolarized	0	0	off

3.1.2   Deuteron polarization

Deuteron is a spin-1 particle for which one can define vector and tensor polarizations. The vector and tensor polarization are defined as:

$$p_z = \frac{N_+ - N_-}{N_+ + N_- + N_0}, \tag{3.1}$$

$$p_{zz} = \frac{N_+ + N_- - 2N_0}{N_+ + N_- + N_0}, \tag{3.2}$$

where $N_{+,0,-}$ is the population of particles in the substates with $m = +1$, 0 and -1, respectively. Deuterons with pure vector polarization can be obtained using a weak field of 7 MHz and two strong fields of 455 MHz and 331 MHz, the so-called SFI and SFII, respectively. As shown in Fig. 3.2, the weak field transition gives $p_z = -2/3$ and $p_{zz} = 0$, while applying both strong fields together yields $p_z = +2/3$ and $p_{zz} = 0$. To obtain pure tensor polarization, another transition unit called mean field (MF), residing between the two hexapoles, is used. The mean field induces a transition with $(\Delta J = 0, m_J \rightarrow -m_J)$. The second hexapole after MF is used again to focus atoms with $(m_j = +1/2)$ and defocus $(m_j = -1/2)$. Behind this hexapole, the atomic beam consists of atoms with $m = -1$ and 0. With this MF, using SFI or SFII now yields pure tensor polarization with $(p_z = 0$ and $p_{zz} = +1)$ or $(p_z = 0$ and $p_{zz} = -2)$, respectively. The polarization scheme used in this experiment is summarized in table 3.1. The polarizations mentioned in the table are theoretical values and difficult to achieve in practice. The polarizations which were obtained during the experiment are typically 60-80% of the theoretical values. The analysis results will be discussed in the next chapter.

3.2   The AGOR accelerator

The Accélérateur Groningen ORsay (AGOR) is a second generation cyclotron with superconducting coil [62]. AGOR is capable of accelerating protons, deuterons and

heavy ions. It is a compact three-sector cyclotron with a pole diameter of 1.88 m, equipped with three accelerating electrodes, located in the pole valleys. Protons could be accelerated up to 190 MeV and deuterons with q/A=0.5 to maximum energy of 90 MeV/nucleon at the time of the experiment. These are also the beams used in this experiment.

3.3 The In-Beam Polarimeter (IBP)

The In-Beam Polarimeter (IBP) is used to determine the polarization of proton or deuteron beams, via the H($\vec{p}, p$)p or H($\vec{d}, d$)p elastic reactions, respectively [63]. Its location along the beam line is shown in Fig. 3.1. It consists of 16 Phoswich detectors grouped into four independent planes ($0°, 45°, 90°$ and $135°$); see Fig. 3.3. For example, plane $0°$ is defined as the plane containing the beam axis and the line on which detectors 1, 2, 3 and 4 are placed. In order to reduce the background, inner and outer detectors of each plane are coupled, detecting the ejectile and the recoil of the reaction in time coincidence. For instance, in the plane of $0°$, the detectors numbered 1 and 2 measure in coincidence and are considered as Left, the same for the detectors 3 and 4 which are considered as Right; see table 3.2. This setup is capable of measuring the asymmetry of the reaction, using simply the left-right asymmetry. The measured asymmetry is directly related to the analyzing power of the reaction and the polarization of the incoming beam. Knowing the analyzing power, the polarization of the incoming beam can be obtained from:

$$p = \frac{A_s}{A_y}, \tag{3.3}$$

where A_y is the specific analyzing power of the reaction, A_s is the asymmetry and p is the related beam polarization. In the case of the proton beam, the plane of $0°$ measures the y-component of the polarization and the plane of $90°$ the x-component. In principle, these two planes can work independently. Although the two other planes of $45°$ and $135°$ seem to be redundant, they have been used to extract the value and the direction of the beam polarization more precisely; see Sec. 4.1.1. To measure the tensor polarization, the detectors of two planes, say $0°$ and $90°$, are needed at the same time. The method of analyzing the IBP data will be discussed in chapter 4.

3.4 The Big-Bite spectrometer (BBS)

The Big-Bite Spectrometer (BBS) is a QQD-type (Quadrupole-Quadrupole-Dipole) magnetic spectrometer with a solid angle of up to 13 msr and 430 MeV K-value [64].
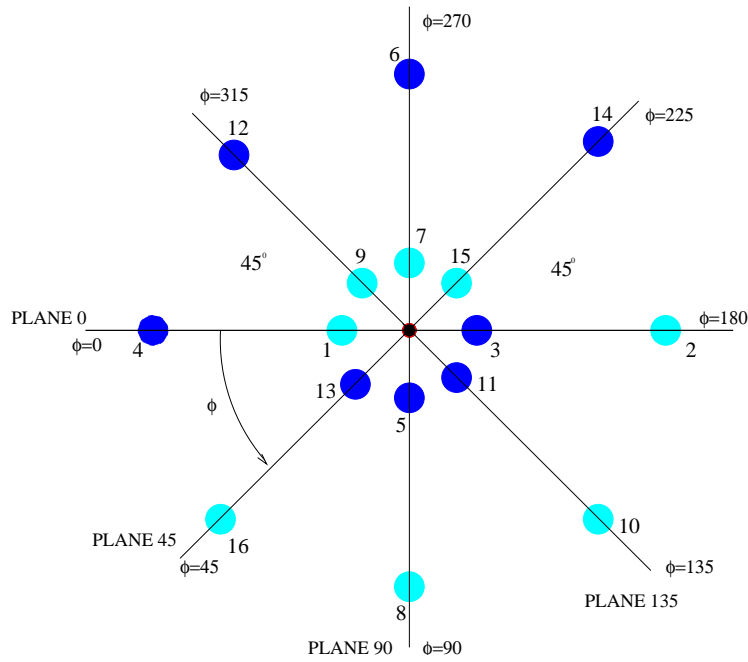
Figure 3.3: A schematic cross-sectional view of the IBP detector. The ϕ-angles are in degrees.

Table 3.2: Relation between the azimuthal angle ϕ and the IBP planes.

Plane	ϕ
$0°$	$0°(\mathbf{L}\text{eft})/180°(\mathbf{R}\text{ight})$
$45°$	$45°/225°$
$90°$	$90°(\mathbf{D}\text{own})/270°(\mathbf{U}\text{p})$
$135°$	$135°/315°$

The BBS can be used in three different modes which are called A, B and C. In these modes the quadrupole doublets are placed at three different distances from the dipole, while the target-dipole distance is fixed. Putting the quadrupoles closer to the target gives a bigger solid angle at the cost of a smaller momentum bite. For this experiment the mode 'B' was used. Table 3.3 shows the design parameters for mode B. More details about the spectrometer can be found in [64, 65, 66]. A top view of the BBS and its detectors are shown in Fig. 3.4.

Table 3.3: Design parameters of the BBS in mode B.

Max. solid angle	9.2 msr
Max. horizontal opening angle	66 mrad
Max. vertical opening angle	140 mrad
Momentum bite $\Delta p/p_0$	19%
Dispersion D	2.54 cm/%
Horizontal magnification M_x	−0.45
Vertical magnification M_y	−10.1
Bending limit	430 MeV
Optimum resolution $\Delta E/E$	4×10^{-4}
Radius of curvature	220 cm
Max. dipole field	1.4 T
Distance target-entrance aperture	81.7 cm
Distance target-entrance Q1	114 cm

3.5 BBS detector system

The detection system developed by the EuroSuperNova collaboration consists of several position-sensitive detectors and two scintillator planes, shown in Fig. 3.4. In the following sections we will discuss the various aspects of the detectors.

3.5.1 Focal-Plane Detection System (FPDS)

There are two Vertical Drift Chambers (VDC) mounted parallel to the focal plane of the BBS. This kind of high-resolution position-sensitive detector was first developed to be used with spectrometers [67]. The VDCs are separated by 23 cm along the central ray with which they form an angle of 39°, see Fig. 3.4. Each chamber has an X and a U wire-plane. The geometrical parameters of the VDCs are listed in table 3.4. The sense wires, which carry a positive high voltage, are read out by time-to-digit converters (TDCs). The VDCs are filled with a gas mixture of 50% argon, as counting gas, and 50% isobutane, as quenching gas. Traveling particles which cross through a VDC ionize the argon atoms. The released electrons are accelerated toward the positively-biased sense wires, producing more ionizations. This causes an avalanche of charge which can be read out by the sense wires. Since the traveling particles pass the VDC obliquely, they can produce several avalanches, absorbed by adjacent wires. By measuring the arrival times of the pulses against a common reference, one obtains a distribution of drift times from which the intersection point

FPDS   FPP

D

220 cm

Q2

Q1

target

2107   621   324   270   270

VDCs 1 and 2
MWPCs D1–D4
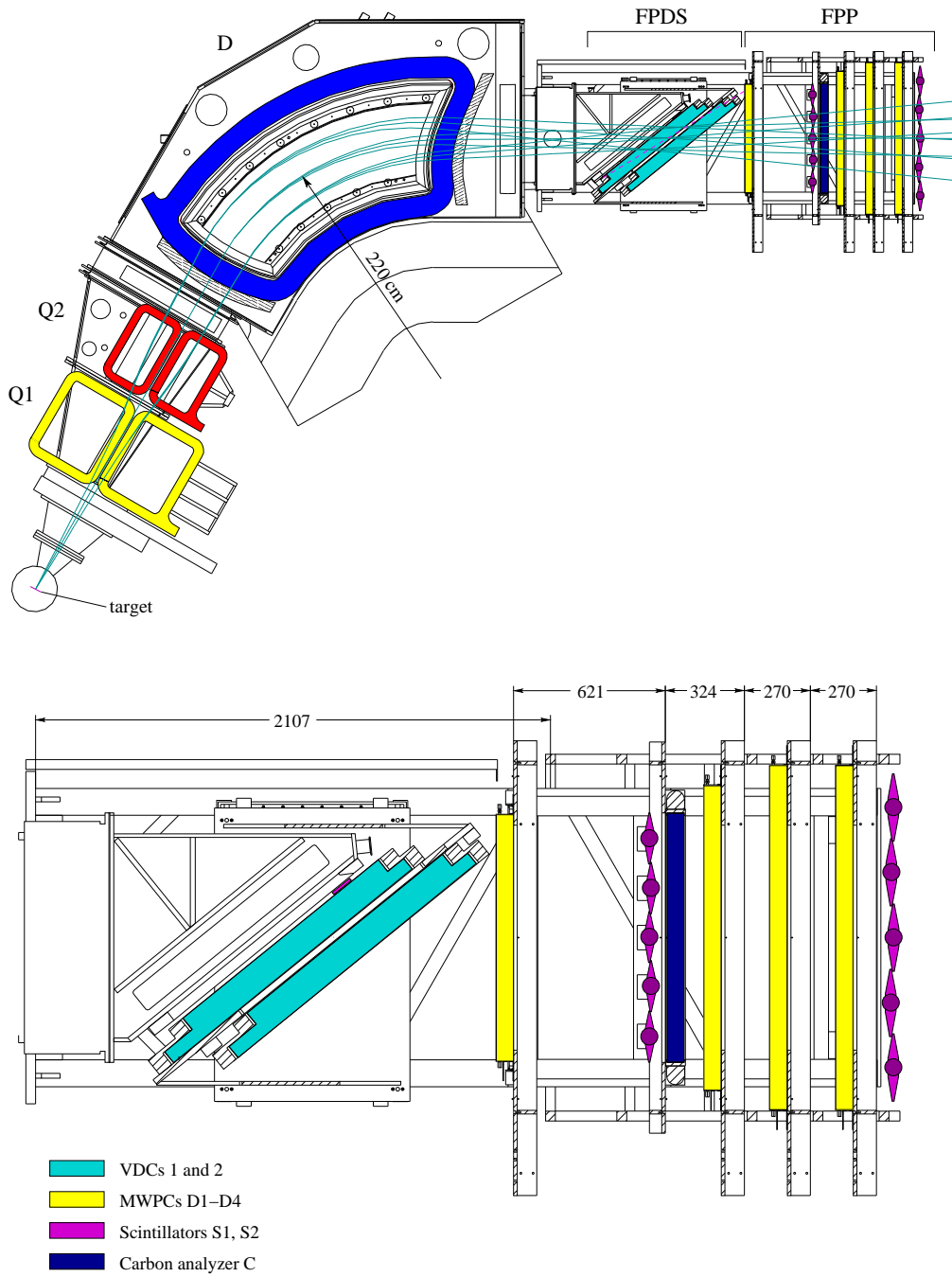Scintillators S1, S2
Carbon analyzer C

Figure 3.4: Top view of the BBS/ESN (top) and the ESN detector (bottom). A few possible particle trajectories are shown. Particles with equal momentum entering the BBS dipole magnet are focused to the same position in the focal plane, regardless of their initial direction.

Table 3.4: Geometrical parameters of the VDCs.

Active detection area	1030×367 mm^2
Angle between VDCs and BBS central ray	39°
Number of sense wires in X planes	240
Number of sense wires in U planes	240
Tilt angle of U plane wires	32.86°
Average cluster size for X planes	9
Average cluster size for U planes	7.5
Sense-wire spacing	4.2 mm
Guard-wire spacing	4.2 mm
Sense-wire thickness	20 μm
Guard-wire thickness	50 μm
Distance wire plane to cathode foil	15 mm

of the particle track and the wire plane can be calculated [67]. The signals of the sense wires are read out by LeCroy 3377 pipeline TDCs which are capable of converting and storing up to 16 signals per channel. The drift times were recorded over a time window of 350 ns.

3.5.2 Focal-Plane Polarimeter (FPP)

In order to measure the polarization of the particles entering the BBS, a polarimeter has been mounted downstream of the FPDS. The polarimeter consists of four Multi-Wire Proportional Chambers (MWPC) and a carbon slab. The polarimeter is based on the measurement of azimuthal asymmetry of a secondary scattering from the graphite slab. The carbon slab is placed after D1, and before D2, D3 and D4 as shown in Fig. 3.4. The geometrical parameters of the MWPCs are listed in table 3.5. Each MWPC has an X and a Y plane of wires. The MWPCs are filled with a mixture of 50% argon and 50% isobutane. The wires are kept at zero potential and a negative high voltage is applied to the cathode foils. They are positioned perpendicular to the central ray and on average one or two wires produce a signal when a particle is passing through them. The signal of the wires are read out by the LeCroy PCOS III system. This system only returns information about the number of hit wires in an event by which the value of the central hit and the size of cluster created by the track can be calculated.

The redundant information of three detectors (two VDCs and D1) before and three detectors (D2, D3 and D4) after the carbon analyzer can be used to fix the

Table 3.5: Geometrical parameters of the MWPCs.

Active detection area MWPC D1	840×400 mm^2
Active detection area MWPC D2	1080×520 mm^2
Active detection area MWPC D3 and D4	1240×960 mm^2
Total number of channels	2976
Wire spacing	2.5 mm
Wire thickness	20 μm
Distance wire plane to cathode foil (D1 and D2)	3 mm
Distance wire plane to cathode foil (D3 and D4)	5 mm

problem of missing or ringing wires in the off-line data analysis. Unfortunately, during a part of the experiment, D3 was not operational. Therefore, to fix this kind of problems, another track reconstruction method was used. A track of incoming particle before the carbon slab is reconstructed using the two VDCs and D1. This track is, then, extrapolated to the middle of the carbon slab. The track of outgoing particle is reconstructed by D2 and D4. This track also can be extrapolated to the middle of the carbon slab. In case there are missing or ringing wires in one of the planes, the extra point at the middle of the slab can be used as redundant information. The distance between the incoming and outgoing tracks should be kept within a certain tolerance allowed by resolutions. The quality of this track reconstruction will be discussed in chapter 4.

3.5.3   Scintillators

Two segmented scintillator planes (Fig. 3.4) located before the carbon analyzer, S1, and after the last MWPC, S2, trigger the readout and produce a common stop signal for VDCs. Each plane consists of five overlapping scintillator paddles of NE102A, which are read out at both ends by Philips XP2262 photo-multipliers. The S1 has a thickness of 2 mm to minimize scattering and energy losses. The second plane has a thickness of 6 mm. The output of the photo-multipliers are discriminated by modified Ortec CCF8200 constant-fraction discriminators (CFDs) which produce logic output signals proportional in width to the time over threshold (TOT) of the incoming pulse. Energy deposit in the scintillators is obtained by measuring the width of the CFD signal with TDCs.
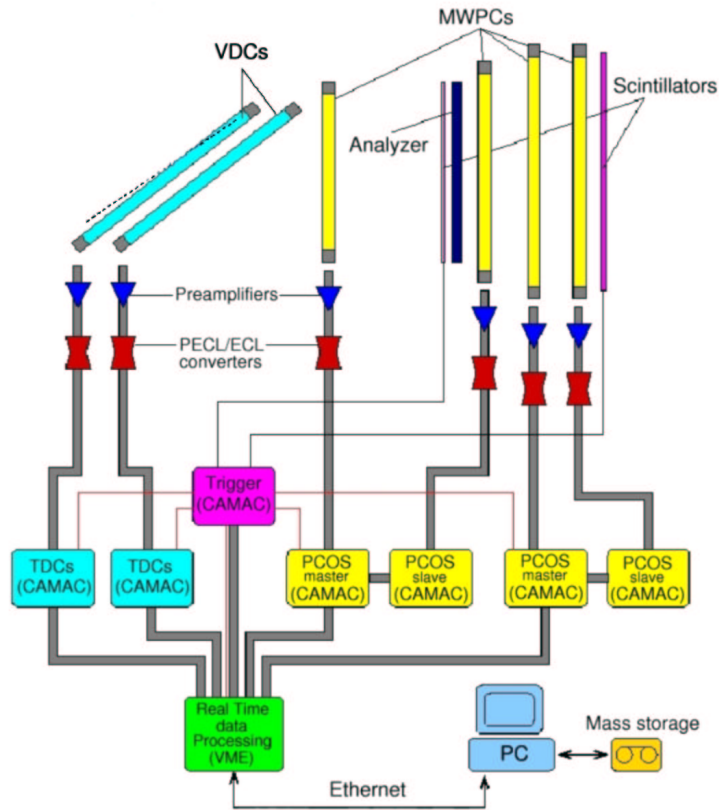
Figure 3.5: Schematic diagram of the read-out of the detection system.

3.6 Electronics

The electronics setup of the ESN detector used during this experiment is shown in Fig. 3.5. It will be described here briefly; more details can be found in [66]. All the wires of the VDCs and MWPCs are read out by preamplifier cards mounted directly on the chambers. One preamplifier board has two Amplifier-Shaper-Differentiator chips with eight channels per chip. The differential logic signals of the chips are converted to ECL signals using PECL/ECL converters. The ECL signals and discriminated signals of the scintillators are read out by CAMAC-based modules. The scintillators and VDCs are read out by LeCroy 3377 TDC modules. Each module contains 32 channels and can store timing information of up to 16 signals per channel. The TDCs of the VDCs are bussed together via ECL front-panel connectors using the LeCroy FERA protocol. The MWPCs are read out by LeCroy PCOS III.

PCOS III delivers the position of the central wire which is hit by the particle and the size of the cluster of wires hit.

The CAMAC units are grouped in five branches which are connected to VME-based real-time data processing. The implemented real-time data-processing system at KVI consists of five first-in-first-out (FIFO) modules, an arbiter and a number of Digital Signal Processors (DSPs) which can be programmed to do some necessary on-line tests. The five CAMAC branches are connected to the front of five FIFOs where the data is buffered. The buffers will be distributed to DSPs by the arbiter. The data will be transfered to a PC where one can visualize them, using on-line data analysis, and save them on disk or a DLT tape for off-line analysis.

The DSPs are programmed to reject the events which have a small scattering angle from the carbon analyzer. Most of the particles scatter to small angles due to Coulomb multiple scattering and only a few percent of particles undergo a hadronic scattering. The calculation performed in the DSPs relies on data from MWPCs. Since during this experiment the MWPC D3 was not working, this option was not used.

Figure 3.6 shows the trigger logic of the system. The trigger is made by coincidence signals from S1 and S2 scintillators. The outputs of CFDs are connected to mean-timers which produce a common output signal for both photo-multipliers connected to top and bottom of the same scintillator paddle. The mean-timer signals of all scintillator paddles of a plane are ORed together. The trigger is made by taking the AND of the two signals from S1 and S2. Moreover, the two signals are connected to TDCs to measure the time-of-flight (TOF) between the two scintillator planes. The trigger signal can be inhibited later by a busy signal of the CAMACs and VME. The advantage of inhibiting the trigger after its creation until the computer is ready to process another event, is that the number of created (primary) versus not inhibited (acquired) triggers, as registered by scalers, gives the dead-time of the read-out system:

$$\text{Deadtime} = 1 - \frac{\text{Acquired events}}{\text{Primary events}} \tag{3.4}$$

The modules are read out and cleared at regular time intervals and upon change of the polarization state of the beam.

3.7   Targets

Part of the experiment, studying both $H(\vec{d}, \vec{p})d$ and $H(\vec{p}, \vec{p})$ reactions, was performed using solid CH_2 targets of various thicknesses. The target thickness for the calibration experiment of $H(\vec{p}, \vec{p})$ was 50 mg/cm^2. For $H(\vec{d}, \vec{p})d$ reaction two targets of
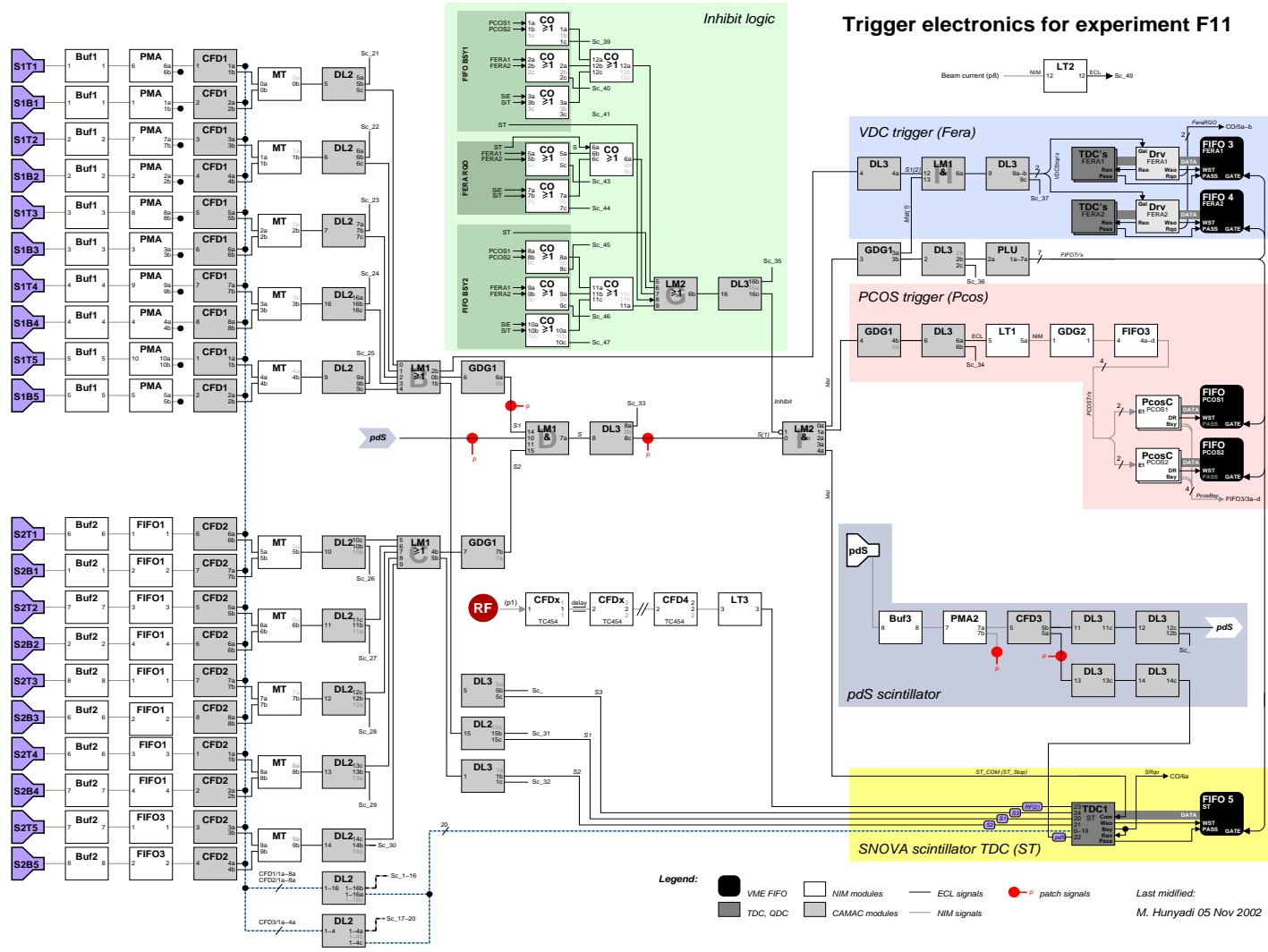
Figure 3.6: Schematic diagram of the trigger logic. The dashed line on top-left represents the position of the focal plane.
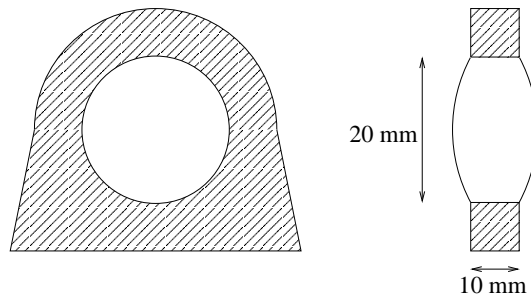
Figure 3.7: The front and side view of the target cell. In the side view the bulging is shown.

109.2 ± 0.3 mg/cm^2 and 194.1 ± 2.2 mg/cm^2 thicknesses were used. The thickness was obtained by measuring the density and the thickness of target around the mark of the beam spot on it.

At the larger angles, where the energy of the scattered particles of the first reaction decreases, the analyzing power of p-C reaction decreases to about 0.1 and lower. Therefore, the figure of merit decreases rapidly; see Sec. 5.1. As a result, the running time would be prohibitively large for these angles. It was decided to use a liquid-hydrogen target for these measurements. Using the liquid-hydrogen target produces much less background as compared to CH$_2$ solid target, since the scattered protons from the carbon in CH$_2$ are considered as background.

The target cells used in the experiments were made of high purity aluminum to optimize the thermal conductivity. Two sizes of cells were used. The thicker cell which was used for H$(\vec{d}, \vec{p})d$ experiment had 20 mm diameter and 10 mm thickness which is corresponding to about 85 mg/cm^2 target thickness including the bulging; see Fig. 3.7. The other cell used in part of the calibration experiment had 16 mm diameter and 6 mm thickness which was about 50 mg/cm^2. The cell together with its gas lead were mounted on a cryogenic cold head which could cool the target cell down to a temperature of around 10 K. The operational target pressure and temperature were chosen to be 190 mbar and 15 K. To decrease the local heating due to the energy loss of the beam particles, the target was mechanically kept in a constant wobbling motion around its center. The foil which was used as target windows was 4 μm synthetic Aramid foil [68]. Using this very thin foil resulted in a low background and minimized the energy loss of the scattered particles in the target. To decrease the energy straggling of the scattered particles in the target, all targets were placed such that the normal vector to the target bisects the scattering angle. Of course, this increased the effective target thickness which was properly accounted for in the analysis.